TECHNICAL NOTES

NATIONAL ADVISORY COMMITTEE FOR AERONAUTICS

CASE FILE COPY

No. 804

WIND-TUNNEL INVESTIGATION OF THE EFFECT OF

VERTICAL POSITION OF THE WING ON THE SIDE FLOW

IN THE REGION OF THE VERTICAL TAIL

By Isidore G. Recant and Arthur R. Wallace
Langley Memorial Aeronautical Laboratory

Washington
April 1941

NATIONAL ADVISORY COMMITTEE FOR AERONAUTICS

TECHNICAL NOTE NO. 804
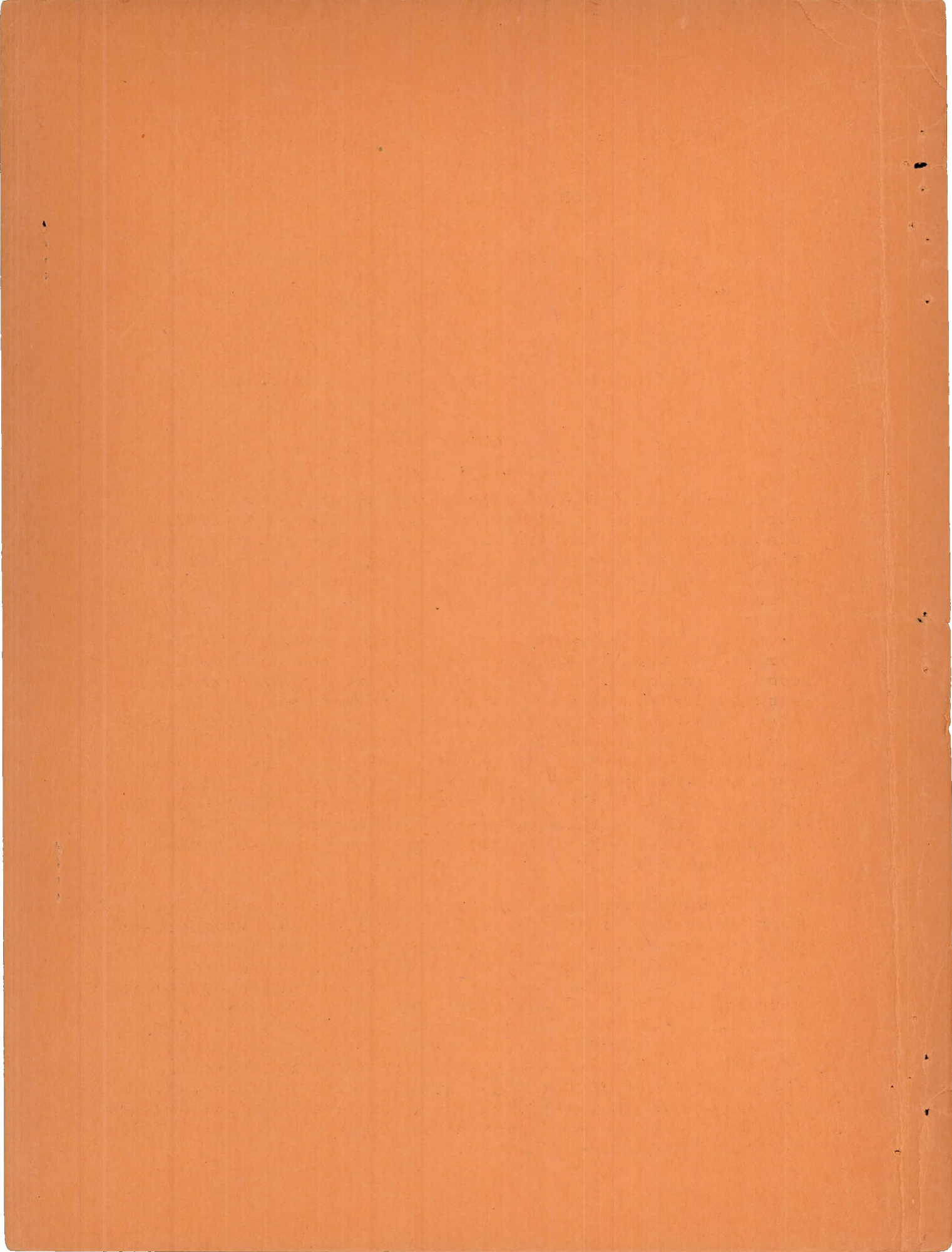
WIND-TUNNEL INVESTIGATION OF THE EFFECT OF

VERTICAL POSITION OF THE WING ON THE SIDE FLOW

IN THE REGION OF THE VERTICAL TAIL

By Isidore G. Recant and Arthur R. Wallace

SUMMARY

An investigation of the air flow at the tail of a monoplane model was conducted in the NACA 7- by 10-foot wind tunnel to determine the cause of the change in vertical-tail effectiveness with a change in the vertical position of the wing on the fuselage and with flap deflection.

Surveys were made of the dynamic pressure and the air-stream angularity in the region of the tail for the combination of a circular fuselage with an NACA 23012 wing having a 3:1 taper ratio and a straight trailing edge. The surveys were made with the wing in high and low positions on the fuselage and with a partial-span split flap deflected and neutral. Similar measurements were made for the wing alone and the fuselage alone. Force tests were also made of the complete model with the vertical tail in place to determine the effect of wing position on the characteristics of the vertical tail at large angles of yaw.

It was found that the yawed wing-fuselage combination produced a side flow which increased the tail effectiveness by increasing the rate of change of vertical-tail angle of attack with a change in the angle of yaw when the wing was in the low position and which tended to decrease the tail effectiveness by decreasing this rate of change when the wing was in the high position. Flap deflection produced a side flow that increased the rate of change of the vertical-tail angle of attack with a change in angle of yaw regardless of wing position. The vertical tail of the low-wing combination gave indications of stall at a smaller angle of yaw than the vertical tail of the high-wing combination.

INTRODUCTION

The National Advisory Committee for Aeronautics is
undertaking an extensive investigation of the lateral-
stability characteristics of airplanes as affected by the
geometrical arrangement of the component parts. The re-
sults of a considerable amount of both theoretical and
experimental research have been published on the deter-
mination of the lateral-stability characteristics of the
component parts of an airplane (references 1, 2, and 3)
and on the application of these characteristics to prac-
tical design (reference 4). The interference effects on
the lateral-stability characteristics have been experi-
mentally determined for certain types of models (refer-
ences 5 and 6).

The data obtained by these wind-tunnel studies in-
dicate that it is not possible to add up the lateral-
stability characteristics of the component parts of the
airplane to obtain the lateral-stability characteristics
of the complete airplane. The aerodynamic interference
produces forces and moments of an appreciable magnitude,
which may exceed the sum of those of the individual
parts. One of the most important of these interference
effects is the change in the forces and the moments con-
tributed by the vertical tail with the vertical wing po-
sition and with the flap deflection. For example, it was
found that the same vertical tail was about twice as ef-
fective when the wing was in a low position as it was
when the wing was in a high position.

The present report describes results obtained from
wind-tunnel tests to determine the cause of the change
in stability contributed by the vertical tail with a geo-
metric arrangement of the model. Analysis of the results
of reference 6 indicates that the change in the contribu-
tion of the vertical tail with vertical wing position and
with flap deflection was probably caused by changes in
the dynamic pressure at the tail and in the angle of at-
tack of the tail. Surveys were therefore made of the
dynamic pressure and the air-stream angularity in the
region of the vertical tail for the combination of the
circular fuselage and the straight trailing-edge wing of
reference 6. Because it was thought that the interference
may influence the stalling characteristics of the vertical-
tail surfaces, force tests were also conducted through a
large range of angles of yaw.

MODEL AND APPARATUS

The model tested is a combination of the circular fuselage and the straight trailing-edge wing used in the tests of reference 6. (See fig. 1.) The wing, which is fully described in reference 3, has an NACA 23012 profile, is tapered 3:1, has its maximum upper-surface ordinates in one plane, and is not twisted. The dihedral angle of the plane of the section chord lines exclusive of the tip portion is 1.45°. The wing area is 4.101 square feet and the aspect ratio is 6.097. The angle of sweepback, measured to the line of section quarter-chord points, is 14°. It was set at 0° incidence to the fuselage center line.

The vertical tail is of NACA 0009 section and has an area of 53.7 square inches, which includes the part of the fuselage shown in figure 1. The aspect ratio of the tail, based on this area and a tail span measured from the fuselage center line, is 2.2.

The 20-percent-chord split flap, made of 1/16-inch steel plate, was attached to the wing at an angle of 60° and extended over 60 percent of the span at the center section. For the high-wing position the center section of the flap was cut away to allow for the fuselage and the gap between the fuselage and the flap was sealed.

The tests were made in the NACA 7- by 10-foot wind tunnel with the regular six-component balance. The closed-throat tunnel is described in reference 7 and the balance is described in reference 8.

The dynamic pressure and the air-stream angularity were measured with a bank of pitot-yaw tubes connected to a direct-reading multiple-tube manometer. The bank of pitot-yaw tubes was so mounted as to be easily moved over a considerable distance in any direction with respect to the model.

TESTS

The tests were made at a dynamic pressure of 16.37 pounds per square foot, which corresponds to a velocity of about 80 miles per hour under standard conditions.

The test Reynolds number was about 609,000 based on a
mean chord of 10 inches. Because of a turbulence factor
of 1.6 for the tunnel, the effective Reynolds number was
about 975,000.

The surveys of dynamic pressure and air-stream angu-
larity were made with the vertical tail removed and with
the model at an angle of attack of 0° and angles of yaw
of -5°, 0°, and 5°. The zero angle of attack was consid-
ered representative because the tail effectiveness did
not vary greatly with angle of attack. The model arrange-
ments for which surveys were made included the fuselage
and the wing separately and in combination as a high-wing
and a low-wing monoplane. All combinations involving the
wing were tested with the flap deflected and neutral.

The surveys were made in two planes. One plane was
vertical at an assumed rudder-hinge position 25.6 inches
behind the assumed center of gravity of the model (plane
B, fig. 1); the other plane was parallel with and 1/2
inch behind the leading edge of the vertical tail (plane
A, fig. 1). Both planes were fixed with respect to the
tunnel because the vertical tail of the model moved for-
ward only a negligible amount when yawed to 5°. Horizon-
tal elements of both planes were perpendicular to the air
stream. Measurements were made over a distance of 6 inches
on each side of the vertical center line of the tunnel in
1/2-inch increments. Vertical positions of the survey
planes are indicated in figure 1.

Supplementary surveys of the air-stream angle were
made at 0° angle of attack and 10°, 15°, 20°, and 25°
angles of yaw for the low-wing combination with the flap
neutral and deflected 60°. These surveys were made on a
cross-tunnel line 2.26 inches above the fuselage center
line, and the pitot-yaw tubes were moved slightly forward
with increasing angle of yaw to keep them in line with the
assumed rudder-hinge position.

Force tests were also made at angles of attack of 0°,
5°, 10°, 12°, and 14° for flap neutral and at -5°, 0°, 5°,
8°, and 10° for flap deflected 60°. At each angle of at-
tack the model was yawed through a range of -10° to 50°.
Both low-wing and high-wing combinations with the vertical
tail in place were tested in this manner.

RESULTS AND DISCUSSION

The data, with primes to indicate wind axes, are given in standard nondimensional coefficient form. The coefficients for the fuselage are based on the dimensions of the wing.

$C_Y{}'$ lateral-force coefficient (Y'/qS)

$C_n{}'$ yawing-moment coefficient (N'/qSb)

where

Y' lateral force

N' yawing moment

S wing area

b wing span

q free-stream dynamic pressure $(1/2\ \rho V^2)$

and

A aspect ratio

q_t dynamic pressure in region of tail

l tail length

α angle of attack, degrees

ψ' angle of yaw, degrees

σ sidewash angle, degrees, measured from wind axis (positive when it tends to decrease the angle of attack of vertical tail)

$C_n{}'_\psi$ partial derivative of $C_n{}'$ with respect to ψ'

$C_Y{}'_\psi$ partial derivative of $C_Y{}'$ with respect to ψ'

$\left(\dfrac{dC_L}{d\alpha}\right)_t$ slope of vertical-tail lift curve with respect to angle of attack

The subscript t refers to the tail.

The forces and the moments are given with respect to the wind axes that intersect at the center-of-gravity location shown in figure 1.

Precision.- The measurements taken are believed to be within the following limits of accuracy:

α . . . . $\pm 0.1^{\circ}$

ψ' . . . . $\pm 0.2^{\circ}$

σ . . . . $\pm 1/4^{\circ}$

C_Y' . . . . ± 0.001

C_n' . . . . ± 0.0002

q_t/q . . . . ± 2 percent

Force-test data.- Force-test data of the model and its component parts are presented in reference 6, and the results for $\alpha = 0$ are summarized in table I. From the data of table I the contributions of the vertical tail for the several model arrangements have been computed by deducting the values of $C_n'_{\psi}$ and $C_Y'_{\psi}$ for the model without the vertical tail from the values for the model with the vertical tail. These vertical-tail contributions are given in table II.

The data of table II show that the directional stability $C_n'_{\psi_t}$ contributed by the vertical tail in the presence of the high wing with flap neutral is 35 percent less than that contributed by the tail with the wing absent. With the flap deflected 60°, the stability due to the vertical tail of the high-wing combination is 19 percent less than that of the tail with the wing absent. When the wing is in the low position with $\delta_f = 0^{\circ}$ and 60°, the directional stability contributed by the vertical tail is 35 and 56 percent, respectively, greater than that contributed by the tail with the wing absent. It may also be noted that, with the wing in either the high or the low position, the deflection of the flap increases the stability contributed by the vertical tail in the presence of the combination, the increases being about 25 percent for the high position and 15 percent for the low position.

The rate of change with the angle of yaw of lateral

force contributed by the vertical tail $C_{Y'_{\psi_t}}$ is also
affected by the wing position and the flap deflection.
With the wing in the high position, $C_{Y'_{\psi_t}}$ is decreased
41 percent and 33 percent when $\delta_f = 0°$ and $60°$, re-
spectively, as compared with $C_{Y'_{\psi_t}}$ with the wing absent.
The low-wing combination increases $C_{Y'_{\psi_t}}$ by about 20
percent when $\delta_f = 0°$ and 44 percent when $\delta_f = 60°$. As
in the case of the directional stability, the lateral
force $C_{Y'_{\psi_t}}$ is increased by flap deflection regardless
of wing position, the increase being about 15 percent for
the high-wing combination and 20 percent for the low-wing
combination.

The yawing moment produced by the vertical tail is
generally assumed to be the force of the tail applied at
some distance from the center of gravity of the model.
Expressed in coefficient form, this moment may be written

$$C_{n'_{\psi_t}} = -\frac{C_{Y'_{\psi_t}} \, l}{b} \tag{1}$$

where l is the length of tail from the center of gravity
of the model to the center of pressure of the tail.

It will be noted from table II that the percentage
change in $C_{n'_{\psi_t}}$ does not correspond to the percentage
change in $C_{Y'_{\psi_t}}$ as required by equation (1), but the
values do correspond as closely as could be expected con-
sidering the experimental error and the possibility of a
small shift in the center of pressure of the tail.

The lateral force contributed by the vertical tail
may be written

$$Y'_t = \left(\frac{dc_L}{d\alpha}\right)_t \alpha_t \, q_t \, S_t = C_{Y'_{\psi_t}} \, \psi' q S \tag{2}$$

or

$$C_{Y'}{}_{\psi_t} = \left(\frac{dC_L}{d\alpha}\right)_t \frac{\alpha_t}{\psi'} \frac{q_t}{q} \frac{S_t}{S} \qquad\qquad (3)$$

The terms S_t, S, ψ', and q were the same for all tests. The term $(dC_L/d\alpha)_t$, which is the slope of the tail lift curve, should be the same for all cases because it is a function mainly of tail section and effective tail aspect ratio. Inasmuch as the data of table II indicate that $C_{Y'}{}_{\psi_t}$ varies considerably with the wing position and the flap deflection, it is logical to conclude that the only remaining quantities, α_t and q_t, must vary with different model conditions.

Dynamic pressure in the region of the tail.- The possibility of a change in dynamic pressure in the region of the tail with a variation in the wing position was first investigated. The results are presented in the form of contours of equal dynamic-pressure ratio q_t/q superimposed on a rear view of the model and are shown in figures 2 to 4. The values of q_t/q shown are averages of measurements made for $\psi' = \pm 5°$.

The fuselage alone reduced the dynamic pressure in the region of the tail. (See fig. 2(a).) The greatest reduction was confined to a region near the surface of the fuselage and was probably caused by the thickening of the boundary layer toward the rear. An average dynamic pressure, weighted according to local chords, was taken on the tail vertical center line. It was found that the dynamic pressure was 8.9 percent below the free-stream dynamic pressure. The wake of the wing alone with the flap undeflected also reduced the dynamic pressure in the region of the tail (fig. 2(b)). When the wing was in the position it would occupy as a high wing, its wake struck the tail near the fuselage-tail juncture. With the low-wing position, however, the entire tail was outside the wake and the dynamic pressure at the tail probably was unaffected by the wing wake. Contours for the wing alone with flaps deflected 60° are not shown but, because the flap deflection lowered the wing wake, the tail dynamic pressure should be less affected by the wing alone with the flap deflected than with the flap neutral.

The effect of the combination of the fuselage and the wing in the high position on the tail dynamic pressure is shown in figure 3. With the flap undeflected (fig. 3(a)),

the additive effect of the fuselage boundary layer and
the wing wake is reflected in the low values of the
dynamic-pressure ratio in the region that would be occu-
pied by the base of the vertical tail. Nevertheless,
the larger portion of the tail area was outside this
region of greatly reduced q_t/q. The weighted average
dynamic pressure was computed to be 12.8 percent below
free-stream dynamic pressure. When the flaps were de-
flected 60° (fig. 3(b)), the wake was lowered and the
tail dynamic pressure was only 4.5 percent below free-
stream dynamic pressure. These percentages, of course,
would be somewhat different for a vertical tail of a dif-
ferent shape and height.

The effect of the combination of the fuselage and
the wing in the low position on the tail dynamic pressure
is shown in figure 4. With the flaps undeflected, there
was a slight reduction of dynamic pressure, practically
the same as for the fuselage alone. The weighted average
shows this reduction to be 8.5 percent below free-stream
dynamic pressure. With flaps deflected 60°, the tail
dynamic pressure was about 2 percent beyond free-stream
dynamic pressure.

From the foregoing discussion it will be seen that
the change in the dynamic pressure at the tail with a
change in the wing position can account for only a small
portion of the change in the tail effectiveness with the
wing position. Even when the wing condition has a maxi-
mum effect on q_t/q (high wing $\delta_f = 0°$), the dynamic
pressure at the tail was reduced only about 12.8 percent.
The inadequacy of the change in the tail dynamic pressure
as an explanation of the change in tail effectiveness is
even more marked in the case of the low-wing combination
for which the tail lift was increased by about 20 percent
while the tail dynamic pressure was reduced slightly.
Thus, because all the other terms of equation (3) have
been accounted for, it appears that the change in tail
effectiveness with wing position must be largely caused
by a change in the angle of attack of the tail with the
wing position.

Sidewash angle at the tail.- The discussion in the
previous sections has indicated that the change in the
tail effectiveness is primarily caused by a change in the
angle of attack of the tail. If this assumption is true,
when the model is set at a given angle of yaw ψ', the
angle of attack of the tail is not ψ', but $\psi' - \sigma$,
where σ is an increment of the angle, and the magnitude

and the direction of σ depend on the wing position and the flap deflection. By analogy with the downwash angle of the horizontal tail, this increment may be termed the "sidewash" angle. The existence of such a sidewash angle, which has been suggested in references 6 and 9, is definitely established by surveys in the region of the tail; the results of these surveys are presented in figures 5 to 12. The probable causes of sidewash will be discussed in a later section.

From the foregoing definition of sidewash angle, the angle of attack of the vertical tail can be expressed as the difference between the angle of yaw of the model and the average sidewash angle

$$\alpha_t = \psi' - \sigma \tag{4}$$

If this value of α_t is substituted in equation (3) and the expression solved for σ, an equation results that will give average sidewash angles

$$\sigma = -\psi' \left\{ \left[\frac{C_{Y'_{\psi_t}}}{\left(\frac{dC_L}{d\alpha}\right)_t} \cdot \frac{q}{q_t} \cdot \frac{S}{S_t} \right] - 1 \right\} \tag{5}$$

The aspect ratio of the vertical tail used in these tests is 2.2. For this aspect ratio the slope of the lift curve for the isolated vertical tail is 0.046 (fig. 3, reference 9). When this value together with the wing and the tail areas is inserted, equation (5) becomes

$$\sigma = -\psi' \left[\left(\frac{C_{Y'_{\psi_t}}}{0.0042} \frac{q}{q_t} \right) - 1 \right] \tag{6}$$

Thus for $\psi' = 5°$, the angle of yaw at which the surveys were made, the sidewash angles were computed and are presented in table III together with weighted averages of measured sidewash angles for comparison.

The computed values of σ are, of course, not exact. They depend on the slope of the lift curve of the isolated vertical tail, which, in turn, depends on the effective aspect ratio. The aspect ratio of the tail in the present case, as has been previously indicated, is based on a rather arbitrary area and span. If, for example, the exposed area of the tail (45 sq in.) and the span at the

assumed rudder-hinge line are used in computing the aspect ratio, there are obtained sidewash angles that are in closer agreement with the measured values. These values are shown in the last column of table III. In any case, the values in table III indicate the direction and the order of magnitude of the sidewash angles to be expected.

Contours of equal measured sidewash angles in the region of the tail for the various model conditions and for angles of yaw of $0°$ and $5°$ are shown in figures 5 to 12. The results for $\psi = 5°$ are averages of measurements made at $\psi = \pm5°$ for each model condition. This procedure, in effect, removes any asymmetry that might have been present at zero yaw. The values for $\psi = 5°$ are therefore not strictly comparable with those for $\psi = 0°$; the values for $\psi = 0°$ have been included only because they indicate the configuration or the pattern of the sidewash angles for the yaw condition of $0°$. (The arrows on the figures indicate the direction of the side flow for positive and negative angles of sidewash.)

At zero angle of yaw (figs. 5 to 8), negative and positive angles of sidewash were, in general, distributed symmetrically with respect to the center line of the tail so that the average angle of sidewash was $0°$, as would be expected. The high-wing combination with $\delta_f = 0°$ or $60°$ appears to give a negative value of sidewash in plane B (figs. 5(b) and 6(b)). This negative value of σ might have been caused by some asymmetry in the model but, in any case, the value is only about $1/4°$, which is within the experimental accuracy of the measurements.

For an angle of yaw of $5°$, the high-wing combination with $\delta_f = 0°$ or $60°$ (figs. 9 and 10) showed σ to be about $0°$ at the tail surface. If the entire region of the tail is considered, however, it appears that positive sidewash angles predominated. It may be reasonably stated, then, that the high-wing combination with the flap either neutral or deflected produced average sidewash angles positive in direction but small in magnitude - probably not more than $1/4°$. There appears to be very little difference in the sidewash on the tail center line between $\delta_f = 0°$ and $\delta_f = 60°$ for the high-wing combination. The maximum value of σ on the tail center line was about $1°$ in each case.

With the low-wing combination yawed $5°$ and with flaps neutral, a considerable amount of negative sidewash was

produced (fig. 11).   The maximum value of σ on the tail
center line was about $-7\frac{1}{2}^{\circ}$ and the average value of σ
weighted according to local tail chord for this condition
was about -3.2° .   When the flaps were deflected (fig. 12),
the maximum value of σ on the tail center line became
as great as -10° while the weighted average value of σ
was about -4.3° .

Note. If the difference in sign of the sidewash angles in-
duced by the high-wing and the low-wing combinations is
considered, it would appear probable that the vertical
tail will tend to stall sooner on a low-wing combination
that on a high-wing combination because, at a given angle
of yaw, the tail on the low-wing combination will be at a
higher angle of attack than the tail on the high-wing com-
bination.

Extra Note. It is of interest to note the concentration of large
negative sidewash angles close to the top of the fuselage
for the low-wing combination.   Presumably, there is a
similar concentration on the bottom of the fuselage for
the high-wing condition.   The indications are that, when
a dorsal fin is used, it should be most effective on the
top of the fuselage for a low-wing airplane and on the
bottom of the fuselage for a high-wing airplane.

Effect of component parts on sidewash angles at the
the tail.- The existence of flow angularity indicates the
presence of a lateral flow that must be caused by the vor-
tex field of the model.   Such a field consists, in part,
of vortices associated with

(a) Basic span-load distribution on wing

(b) Unsymmetrical span-load distribution on wing pro-
        duced by yawed wing

(c) Flap deflection

(d) Development of lateral force on fuselage

(e) Wing-fuselage interference

Qualitative discussions of these effects appear in refer-
ences 6 and 9, but the data presented in the present report
may permit a more quantitative evaluation of their relative
importance in producing sidewash.

The sidewash angles produced by the yawed wing alone with flap undeflected are not shown because the values obtained are negligible if the limits of accuracy of the measurements are considered. This fact would indicate that the sidewash caused by the vortices arising from (a) and (b) may be neglected. It must be remembered, however, that all the present surveys were made at an angle of attack of 0° and an effective dihedral angle of about 2°. The lift and the rolling moment for these angles are very small and, consequently, the strength of vortices caused by (a) and (b) is small. The sidewash produced by these vortices may be appreciable at high angles of attack.

The sidewash angles caused by the wing with the flap deflected 60° are shown in figure 13 for $\psi' = 0^{\circ}$ and in figure 14 for $\psi' = 5^{\circ}$. Because the sidewash resulting from vortices (a) and (b) was negligible, the sidewash shown in these figures was produced almost entirely by flap deflection (vortices (c)). For the yawed condition, the flaps contributed a small amount of negative sidewash, probably about -0.2°. This value is about the same whether the wing is considered as a high-wing or a low-wing monoplane. The presence of the fuselage apparently had some effect on the sidewash produced by the flaps because, in the case of the high-wing combination (figs. 9 and 10), the flaps gave practically no sidewash; whereas, in the case of the low-wing combination (figs. 11 and 12), the flaps gave about 1° of negative sidewash. The sidewash produced by the flaps may be expected to increase somewhat with the angle of attack.

The sidewash produced by the fuselage alone is shown in figure 15 for $\psi' = 0^{\circ}$ and in figure 16 for $\psi' = 5^{\circ}$. The weighted average sidewash angle produced by the fuselage was about -1.8° for an angle of yaw of 5°.

The difference between the sum of the sidewash angles caused by the wing alone and the fuselage alone and that of the wing-fuselage combination might have been caused by the vortices arising from interference between the wing and the fuselage. In the case of the low-wing combination this difference is -1.4° for $\delta_f = 0^{\circ}$ and -2.3° for $\delta_f = 60^{\circ}$. In the case of the high-wing combination the values of this difference are 2.0° for $\delta_f = 0^{\circ}$ and 2.2° for $\delta_f = 60^{\circ}$. Theoretical computations of the sidewash angle, in conjunction with pressure-distribution tests, are planned.

The foregoing analysis indicates that most of the

sidewash is probably caused by the vortices associated
with lateral force on the fuselage and by the vortices
originating from the wing-fuselage interference.

Effect of wing position on vertical-tail effectiveness
at high angles of yaw.- The effect of the wing position
on the stability of the model at high angles of yaw is
indicated in figures 17 to 20, which give the yawing mo-
ment and the lateral-force coefficients of the low-wing
and the high-wing combinations with $\delta_f = 0°$ and $60°$
for an angle-of-yaw range from $-10°$ to $50°$.

The yawing-moment and the lateral-force curves for
the low-wing combination with flap either neutral or de-
flected (figs. 17 and 18) become flat and fall off at
high angles of yaw, an indication that the vertical tail
had probably stalled. The curves for the high-wing com-
bination with flap either neutral or deflected (figs. 19
and 20) show no marked tendency toward falling off. It
is believed that these curves justify the observation made
previously that the vertical tail on the low-wing combina-
tion would tend to stall at a lower angle of yaw than the
tail on the high-wing combination.

The reason for the increase with angle of attack in
the slopes of the yawing-moment curves for the high-wing
combination (figs. 19 and 20) is not at present clear.
Apparently, it was not caused by changes in sidewash or
velocity at the tail with angle of attack because such
changes would have been reflected in increased slopes of
the lateral-force curves. The slopes of the curves of
lateral force, however, do not increase. It may be noted
that, if the center of pressure moves back as the angle
of attack increases, the slopes of the yawing-moment curves
will increase without a corresponding increase in the
slopes of the lateral-force curves.

In the case of the low-wing combination (figs. 17 and
18), the slopes of the lateral-force curves decrease with
angle of attack but the slopes of the yawing-moment curves
show no corresponding variation. Such results would be
obtained if the sidewash decreased with angle of attack
while the center of pressure moved rearward.

With the flap undeflected, the low-wing combination
(fig. 17) shows breaks in the yawing-moment and the lateral-
force curves at $\psi' = 25°$ for angles of attack of $0°$ and
$5°$. The curves for the high-wing combination (fig. 19)

show no definite breaks in the yaw range investigated.
With 60° flap deflection the yawing-moment curves for the
low-wing combination at α = -5° and 0° shows a definite
change in slope at ψ' = 15° (fig. 18). The high-wing
combination with this flap deflection (fig. 20) shows no
definite breaks in the curves. These breaks in the curves
are probably caused by change in sidewash angle with
change in angle of yaw.

The effect of yaw on the sidewash angles produced by
the low-wing combination at α = 0° on a line through the
assumed rudder hinge 2.26 inches above the fuselage center
line is shown in figure 21. With the flap undeflected,
the sidewash angle at the intersection of the survey plane
with the tail center line increases with yaw up to an
angle of yaw of 20°. With further increase in yaw, the
sidewash angle at this point decreases. Under such con-
ditions, the actual angle of attack of the tail at ψ' =
30° may be less than at ψ' = 25° and a break in the
yawing moment and lateral-force curves such as is shown
in figure 17 for α = 0° and ψ' = 30° should occur.
With the flap deflected to 60°, the sidewash angle at the
intersection of the survey plane and the tail center line
increases with yaw up to an angle of yaw of 15°, beyond
which point it remains constant. Thus the angle of at-
tack of the tail rises rapidly with yaw to ψ' = 15°;
further increase in yaw increases the angle of the tail
more slowly because the sidewash angle remains constant.
The indications are that a change in the slope of the
yawing moment and the lateral-force curve should occur
at an angle of yaw of about 15°. Such a change in slope
of the curves for this model condition at α = 0° is
shown on figure 18.

The data presented in figure 21 suggest a further
explanation for the increase in effectiveness of a single
vertical tail over that of a twin tail of the same area
and aspect ratio on a low-wing monoplane if they are
otherwise aerodynamically equivalent. It may be seen that
large angles of negative sidewash are concentrated near
the fuselage in the region which would be occupied by
the single tail. In the region which would be occupied
by the twin tail the sidewash is small or positive. Thus,
at a given angle of yaw the single tail would be at a
higher angle of attack than the twin tail and therefore
would be more effective.

CONCLUDING REMARKS

The present report furnishes experimental data on
sidewash angles at the tail. The change in tail effective-
ness with wing position was caused largely by the change
in the angle of attack of the tail resulting from a side-
wash produced by the wing-fuselage combination. This
sidewash was strongly negative for the low-wing combina-
tion and weakly positive for the high-wing combination.
The wing alone at small angles of attack, with flaps either
deflected or undeflected, produced only a small amount of
sidewash. The deflection of the flaps caused slightly
negative sidewash, whether the wing was in the high or the
low position, and therefore improved the tail effective-
ness. The fuselage itself also produced negative side-
wash and should therefore have a beneficial effect on the
stability contributed by the vertical tail. Much of the
sidewash was produced by the interference between the
wing and the fuselage. This interference may be caused
by the change in the wing lift distribution resulting
from the difference in pressure between the sides of the
yawed fuselage. Because of the difference in sidewash,
it is probable that the tail on a low-wing model will
stall at a smaller angle of yaw than the tail on a high-
wing model.

Langley Memorial Aeronautical Laboratory,
     National Advisory Committee for Aeronautics,
          Langley Field, Va., January 30, 1941.

REFERENCES

1. Pearson, Henry A., and Jones, Robert T.: Theoretical Stability and Control Characteristics of Wings with Various Amounts of Taper and Twist. Rep. No. 635, NACA, 1938.

2. Shortal, Joseph A.: Effect of Tip Shape and Dihedral on Lateral-Stability Characteristics. Rep. No. 548, NACA, 1935.

3. Bamber, M. J., and House, R. O.: Wind-Tunnel Investigation of Effect of Yaw on Lateral-Stability Characteristics. I - Four N.A.C.A. 23012 Wings of Various Plan Forms with and without Dihedral. T.N. No. 703, NACA, 1939.

4. Zimmerman, Charles H.: An Analysis of Lateral Stability in Power-Off Flight with Charts for Use in Design. Rep. No. 589, NACA, 1937.

5. Bamber, M. J., and House, R. O.: Wind-Tunnel Investigation of Effect of Yaw on Lateral-Stability Characteristics. II - Rectangular N.A.C.A. 23012 Wing with a Circular Fuselage and a Fin. T.N. No. 730, NACA, 1939.

6. House, Rufus O., and Wallace, Arthur R.: Wind-Tunnel Investigation of Effect of Inteference on Lateral-Stability Characteristics of Four NACA 23012 Wings, an Elliptical and a Circular Fuselage, and Vertical Fins. Rep. No. 705, NACA, 1941.

7. Wenzinger, Carl J., and Harris, Thomas A.: Wind-Tunnel Investigation of an N.A.C.A. 23012 Airfoil with Various Arrangements of Slotted Flaps. Rep. No. 664, NACA, 1939.

8. Harris, Thomas A.: The 7 by 10 Foot Wind Tunnel of the National Advisory Committee for Aeronautics. Rep. No. 412, NACA, 1931.

9. Pass, H. R.: Analysis of Wind-Tunnel Data on Directional Stability and Control. T.N. No. 775, NACA, 1940.

TABLE I

STABILITY CHARACTERISTICS OF MODEL AND COMPONENT PARTS

[Circular fuselage and tapered wing with straight trailing edge; $\alpha = 0°$; data from references 3 and 6]

Model arrangement	Vertical tail	Flap deflection, δ_f (deg)	$C_{n}{'}_{\psi}$	$C_{Y}{'}_{\psi}$
High wing alone	----	0	-0.00010	0.0001
	----	60	-.00022	-.0020
Low wing alone	----	0	-.00005	.0001
	----	60	-.00025	-.0020
Fuselage alone	Off	----	.00058	.0009
Fuselage and vertical tail	On	----	-.00094	.0055
High-wing combination	Off	0	.00048	.0021
	-do-	60	.00032	.0006
	On	0	-.00050	.0048
	-do-	60	-.00091	.0037
Low-wing combination	Off	0	.00041	.0021
	-do-	60	-.00035	.0027
	On	0	-.00165	.0076
	-do-	60	-.00272	.0093

TABLE II

STABILITY CHARACTERISTICS OF THE VERTICAL TAIL

IN THE PRESENCE OF VARIOUS MODEL ARRANGEMENTS

[Computed from data of table I; $\alpha = 0°$]

Model arrangement	δ_f (deg)	$C_n'{}_{\psi_t}$	$C_Y'{}_{\psi_t}$
Fuselage	----	-0.00152	0.0046
High-wing combination	0 60	-.00098 -.00123	.0027 .0031
Low-wing combination	0 60	-.00206 -.00237	.0055 .0066

div by $\frac{S_{vt}}{S_w}$ to get desired

TABLE III

COMPARISON OF MEASURED AND COMPUTED SIDEWASH ANGLES AT THE TAIL

Model arrangement	δ_f (deg)	$C_{Y'\psi_t}$	σ		
			Measured (deg)	Computed $A_t = 2.2$ $S_t = 53.7$ sq in. (deg)	Computed $A_t = 2.25$ $S_t = 45$ sq in. (deg)
Fuselage	----	0.0046	-1.8	-1.0	-2.1
High-wing combination	{ 0 ⎰ 60	.0027 .0031	.2 .2	1.3 1.1	.6 .4
Low-wing combination	{ 0 ⎰ 60	.0055 .0066	-3.2 -4.3	-2.2 -2.7	-3.5 -4.1

Fig. 1

FIGURE 1.- Drawing of NACA 23012 wing in combination with circular fuselage and tail of NACA 0009 section.

(a)

$q_t/q = 1.00$

(High wing) Distance from center line of fuselage, in.

Distance from center line of fuselage, low wing, in.

Distance from center line of fuselage, in.

Distance from center line of vertical tail, in.
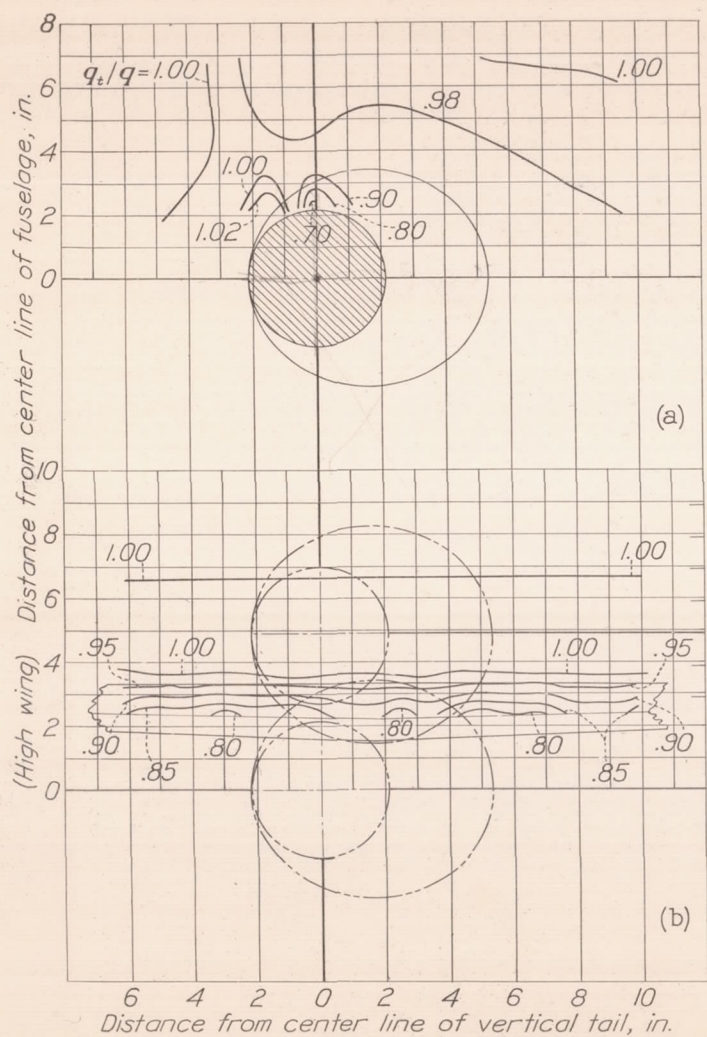
(a) Fuselage alone.   (b) Wing alone, $\delta_f = 0°$.

Figure 2.- Plane A; $\alpha = 0$; $\psi' = 5°$.

Distance from center line of vertical tail, in.
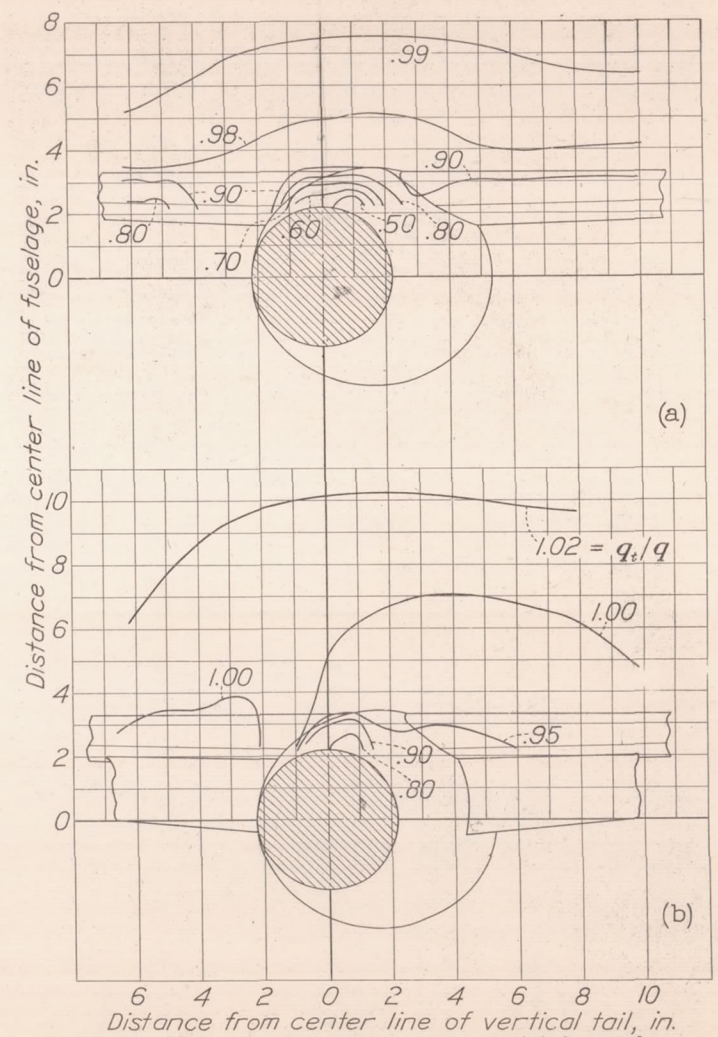
(a) $\delta_f = 0°$.   (b) $\delta_f = 60°$.

Figure 3.- Plane A; $\alpha = 0°$; $\psi' = 5°$; high wing.

Figures 2,3.- Contours of dynamic-pressure ratio, q_t/q, in region of tail.

(a) $\delta_f = 0°$.

(b) $\delta_f = 60°$.
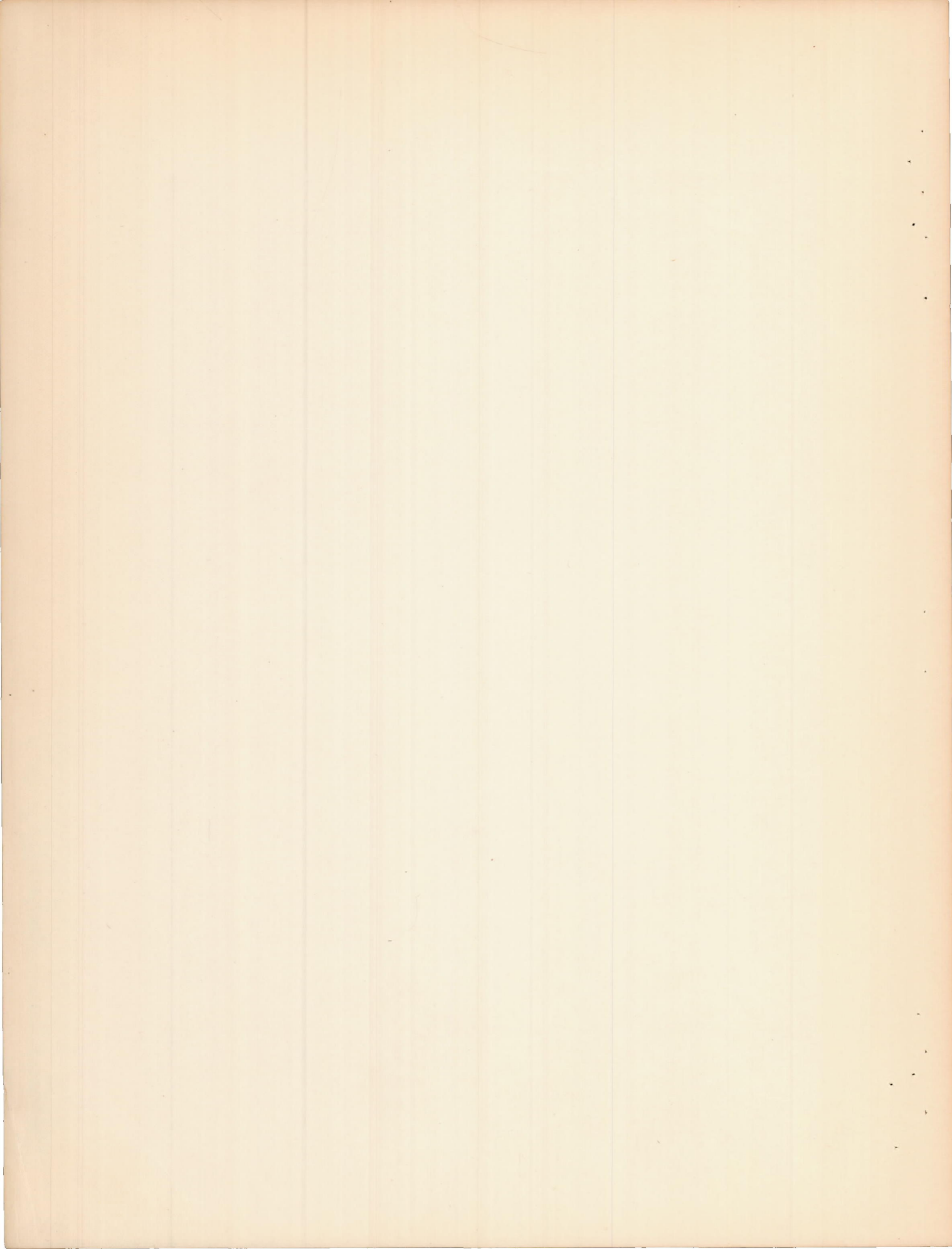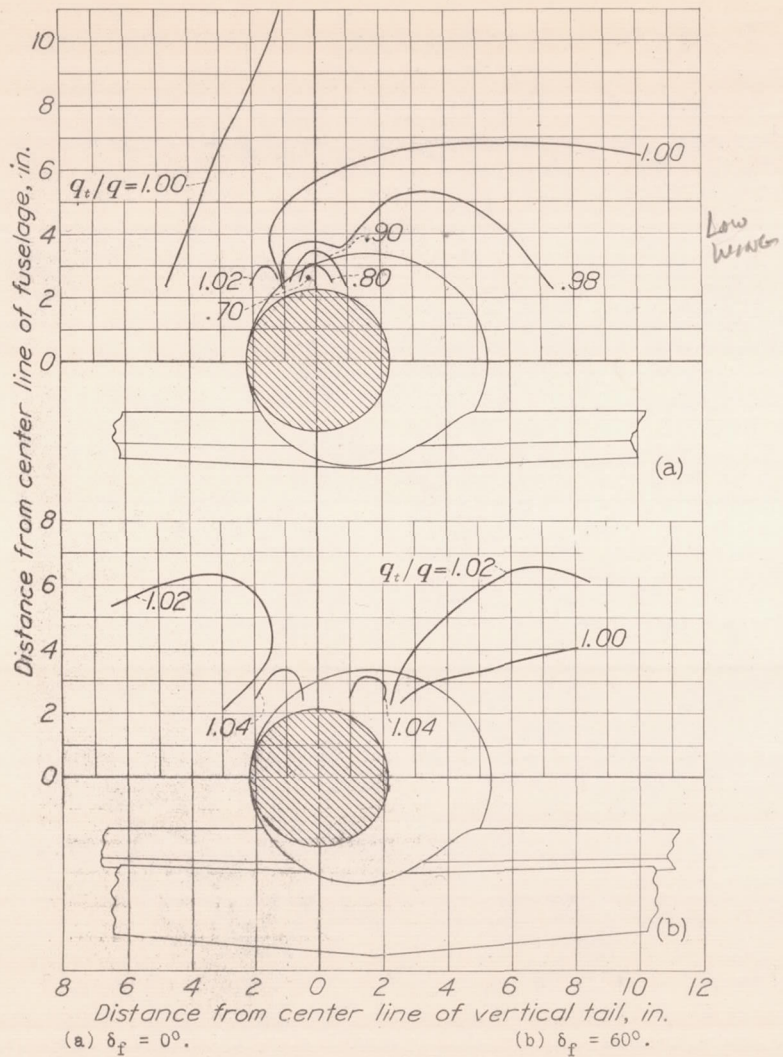
Figure 4.- Contours of dynamic pressure ratio, q_t/q, in region of tail. Plane A; $\alpha = 0°$; $\psi' = 5°$; low wing.
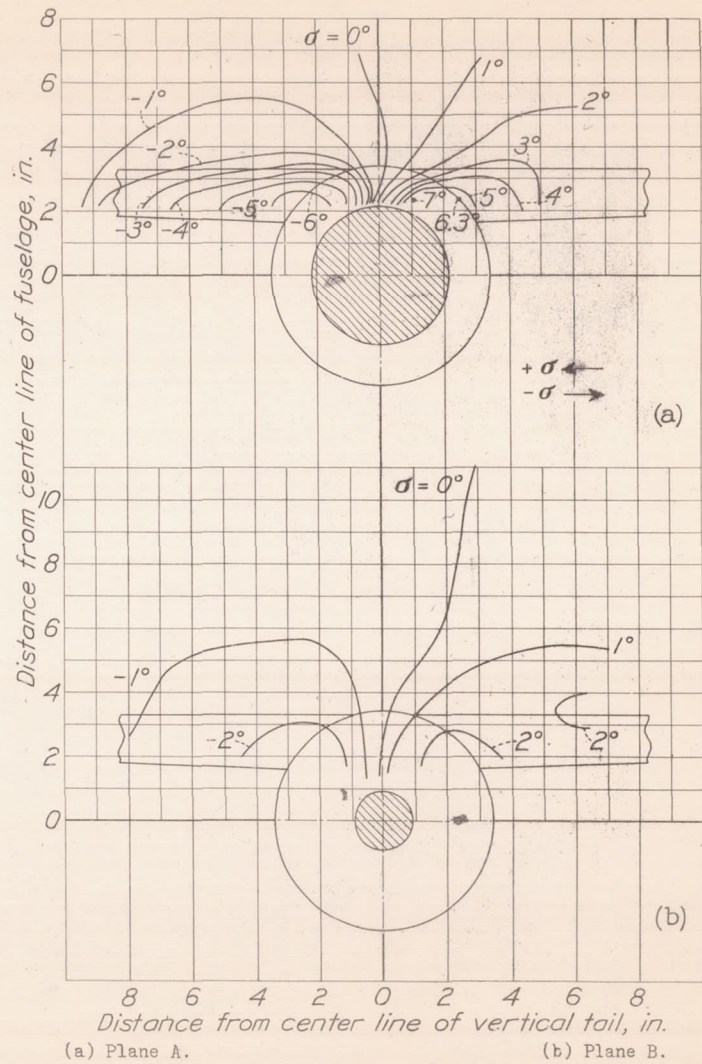
(a) Plane A.

(b) Plane B.

Figure 5.- Contours of sidewash angle, σ, in region of tail. $\alpha = 0°$; $\psi' = 0°$; high wing; $\delta_f = 0°$.
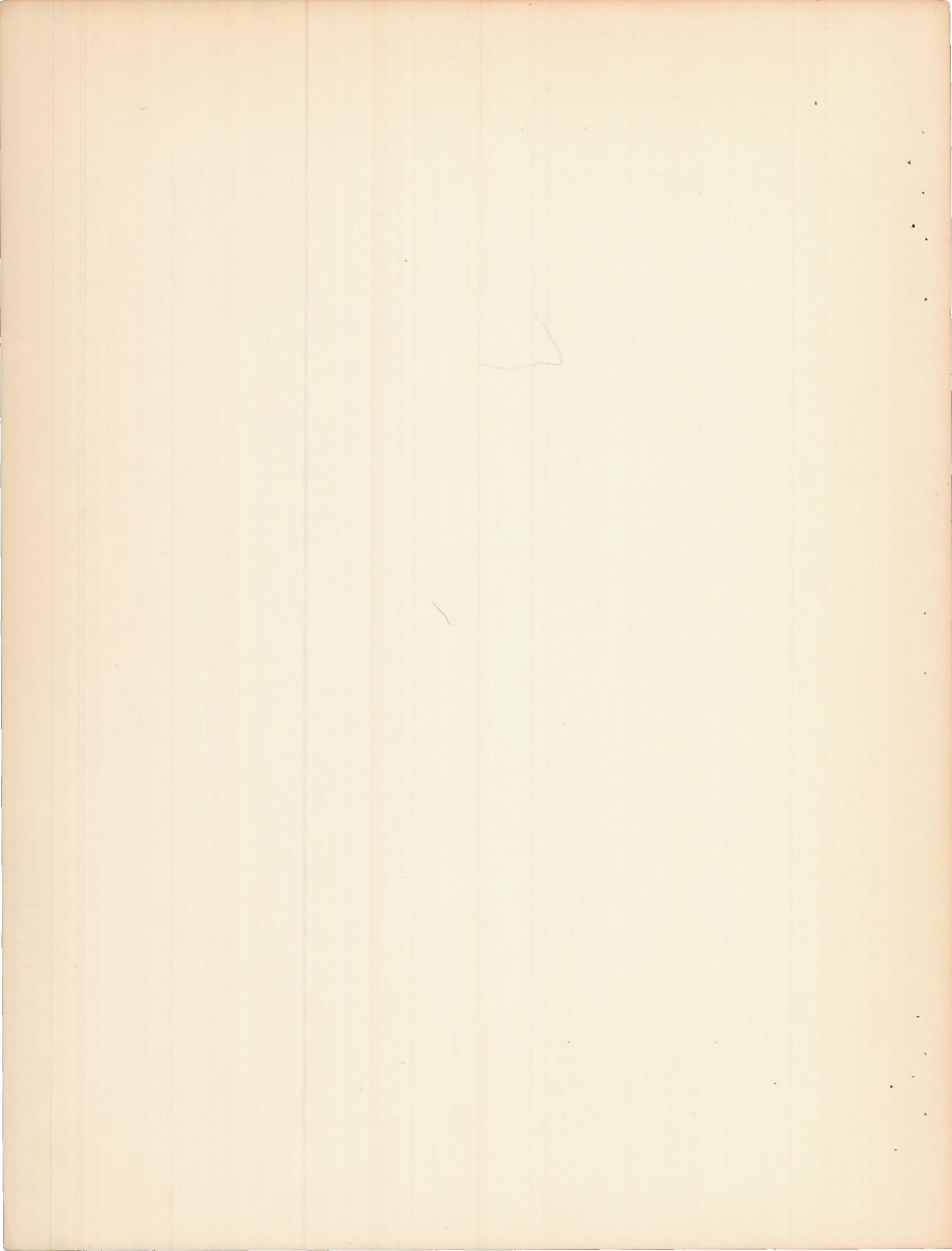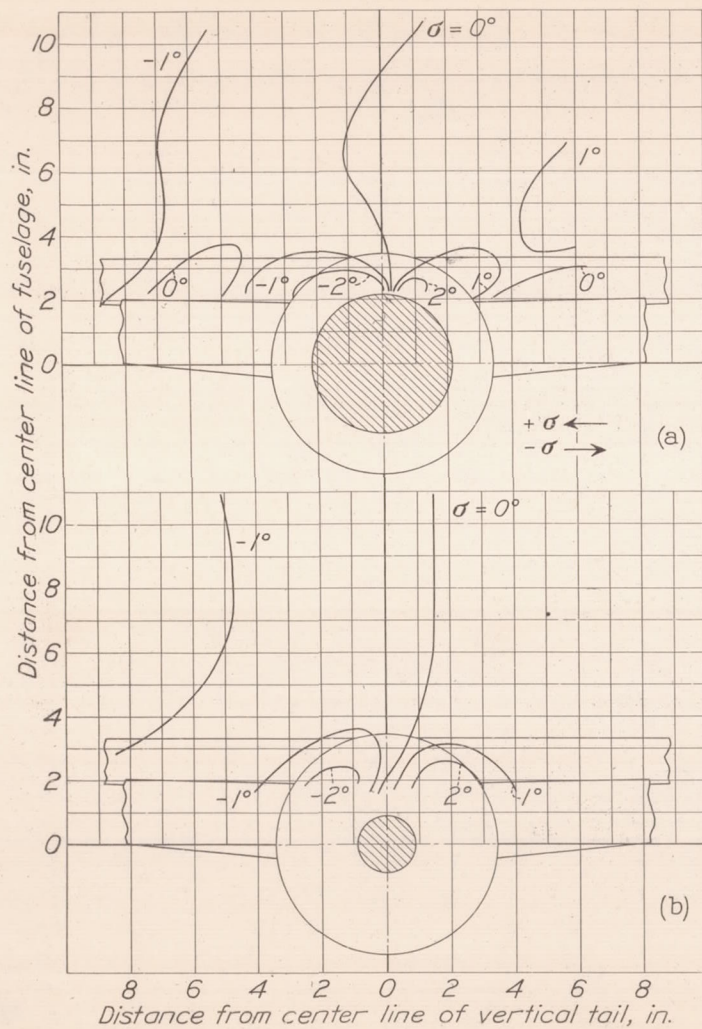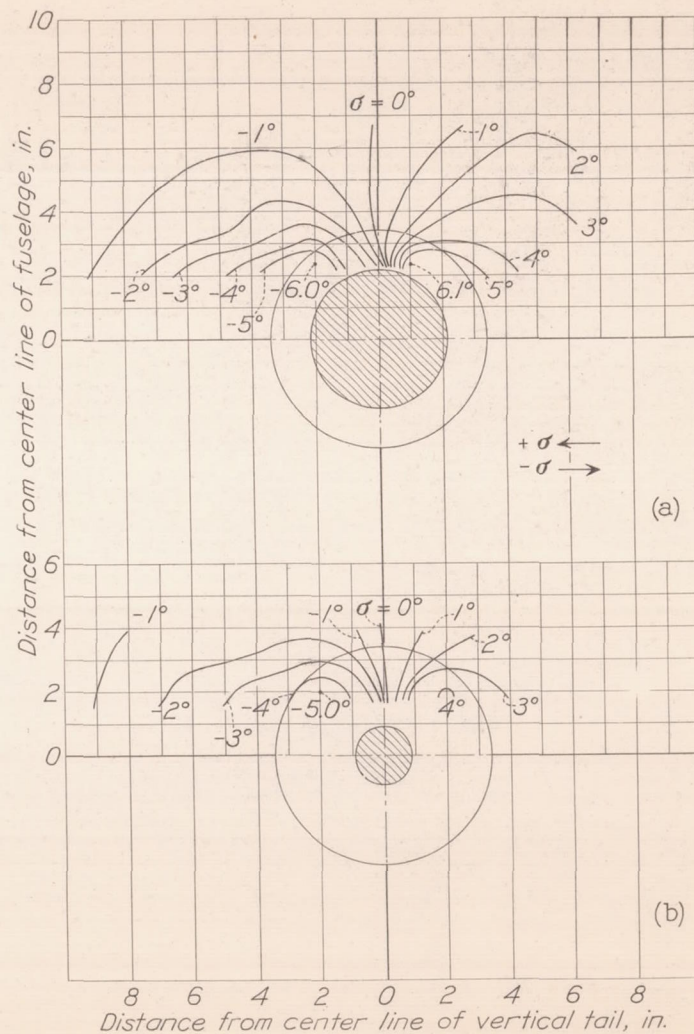
(a) Plane A.   (b) Plane B.
Figure 6.- $\alpha = 0^\circ$; $\psi' = 0^\circ$; high wing; $\delta_f = 60^\circ$.
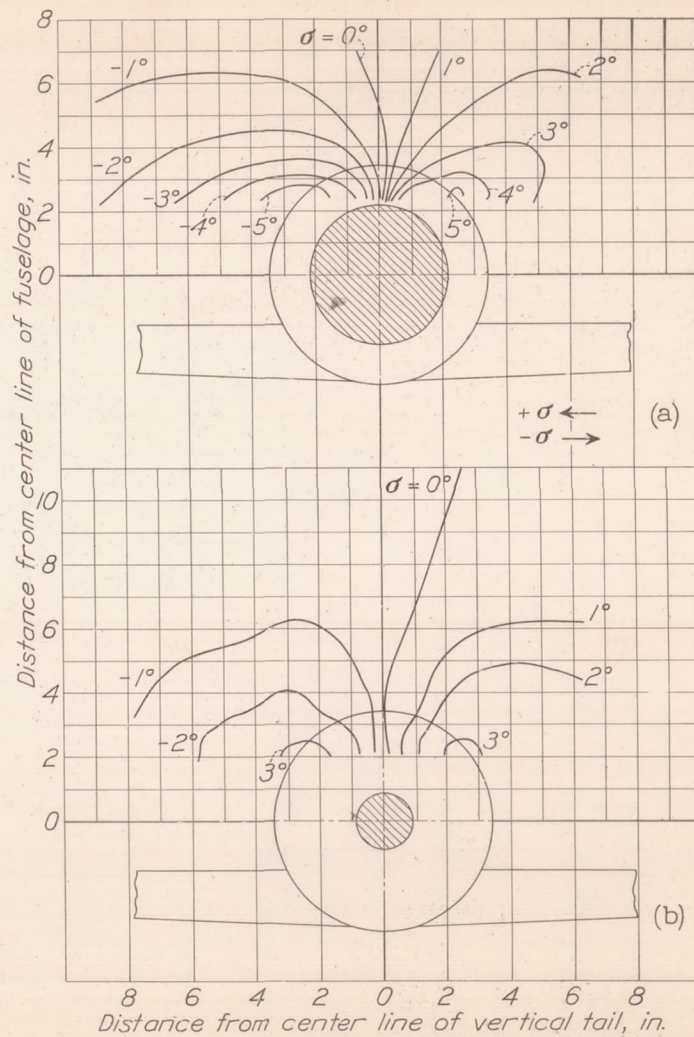
(a) Plane A.   (b) Plane B.
Figure 7.- $\alpha = 0^\circ$; $\psi' = 0$; low wing, $\delta_f = 0^\circ$.

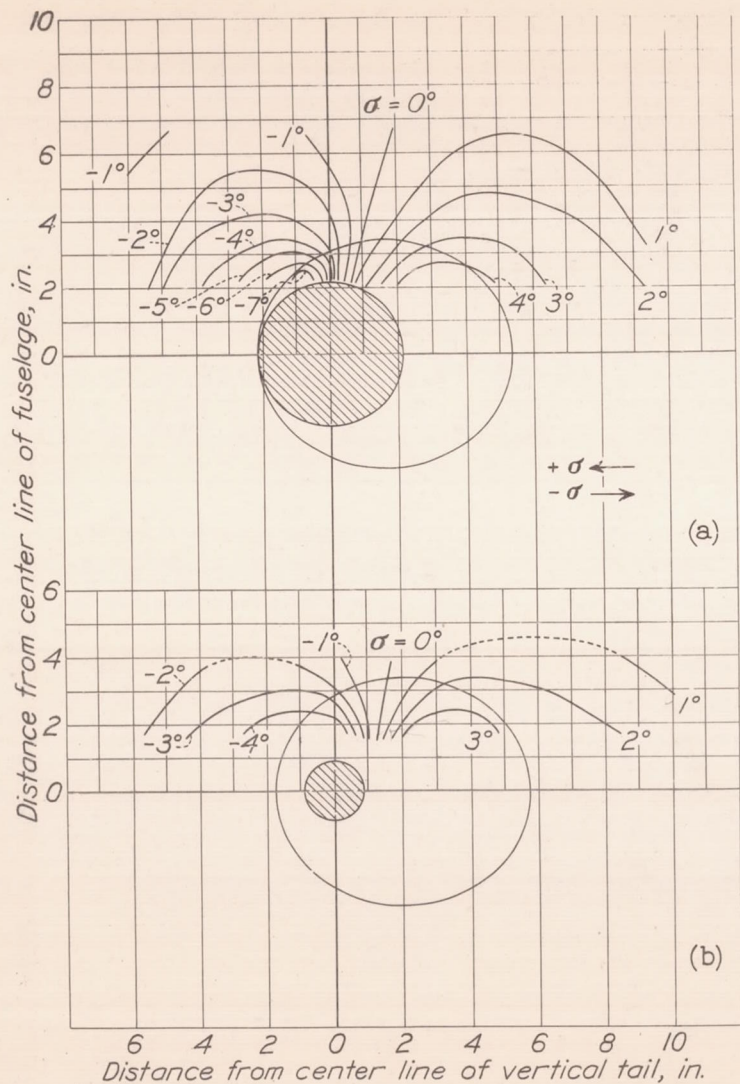Figures 6,7.- Contours of sidewash angle, σ, in region of tail.
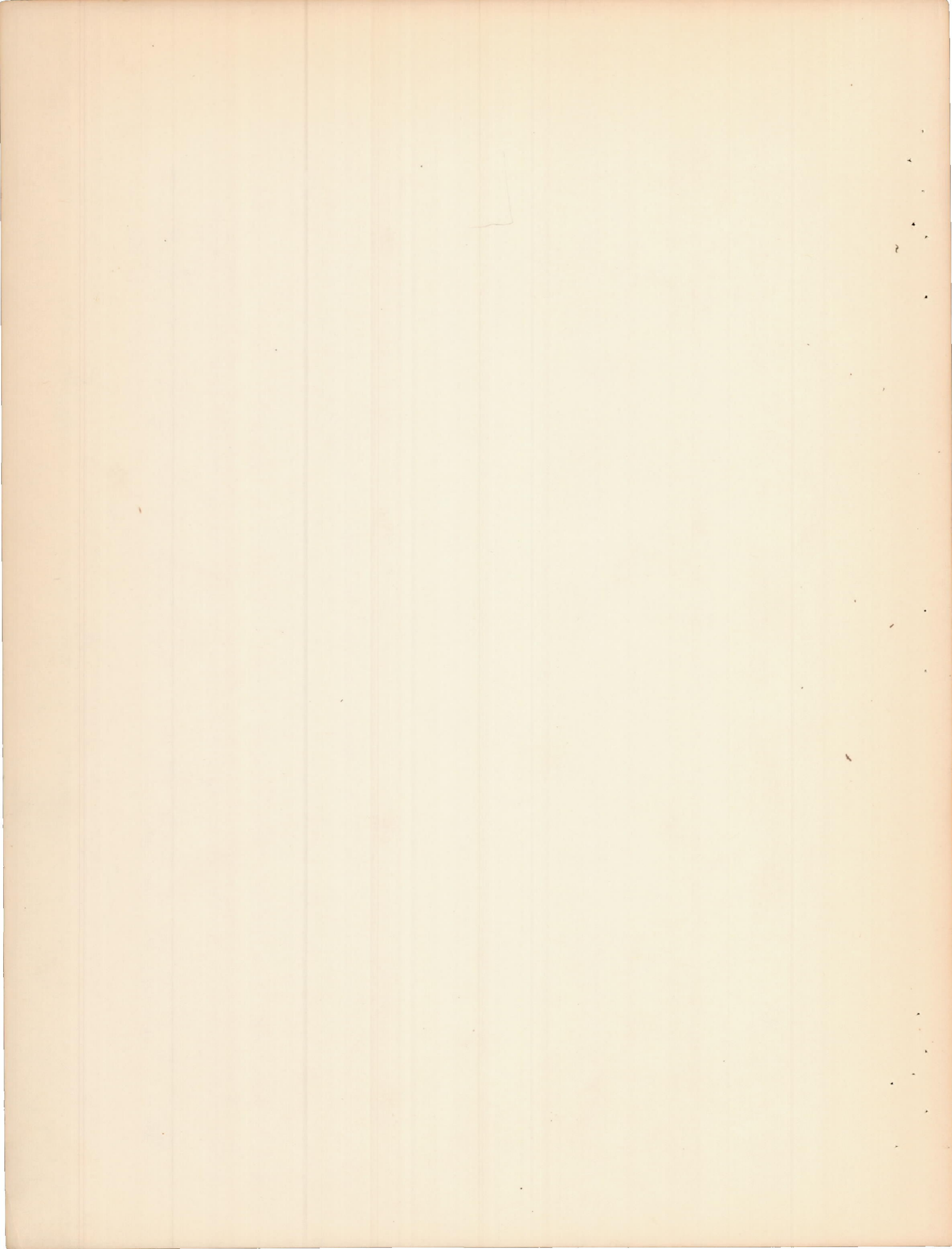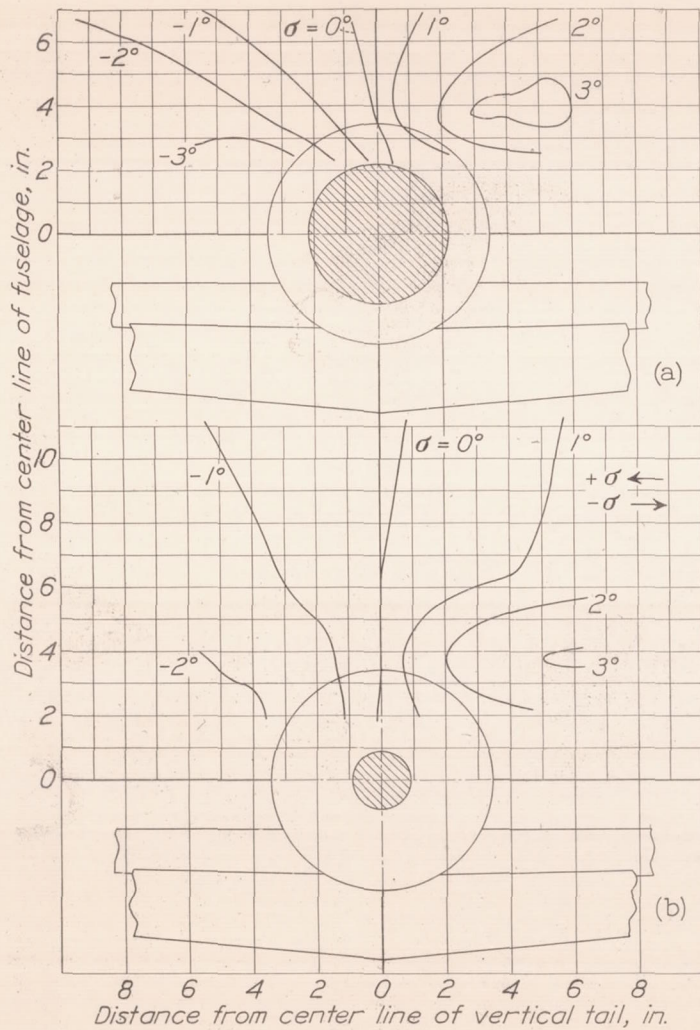
(a) Plane A.   (b) Plane B.

Figure 8.- $\alpha = 0°$; $\psi' = 0°$; low wing; $\delta_f = 60°$.
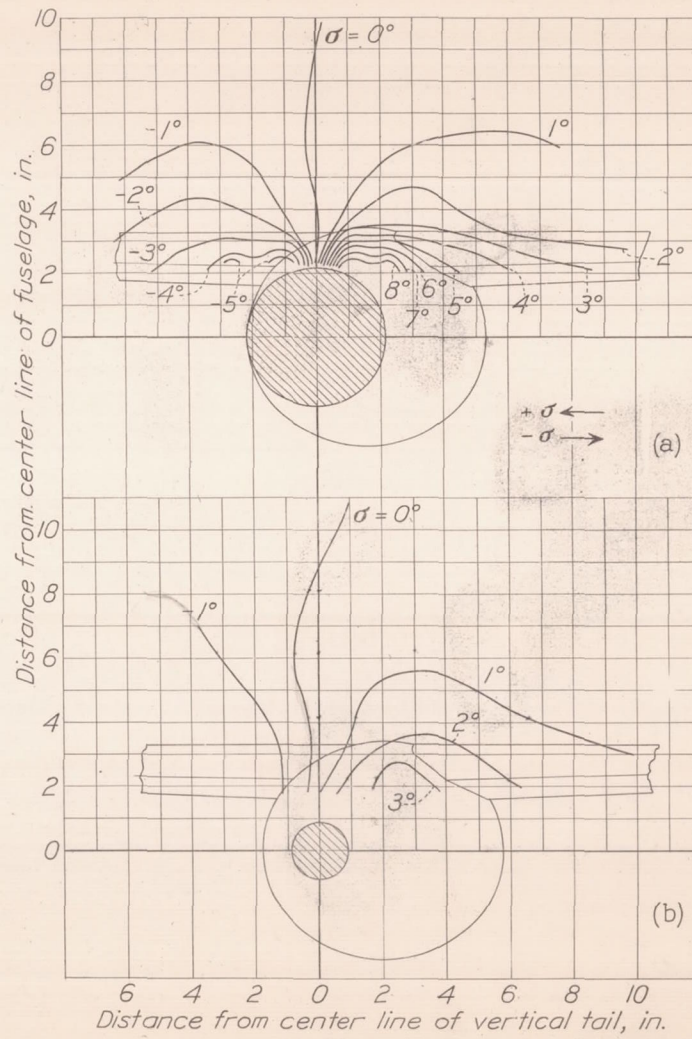
(a) Plane A.   (b) Plane B

Figure 9.- $\alpha = 0°$; $\psi' = 5°$; high wing; $\delta_f = 0°$.

Figures 8,9.- Contours of sidewash angle, σ, in region of tail.
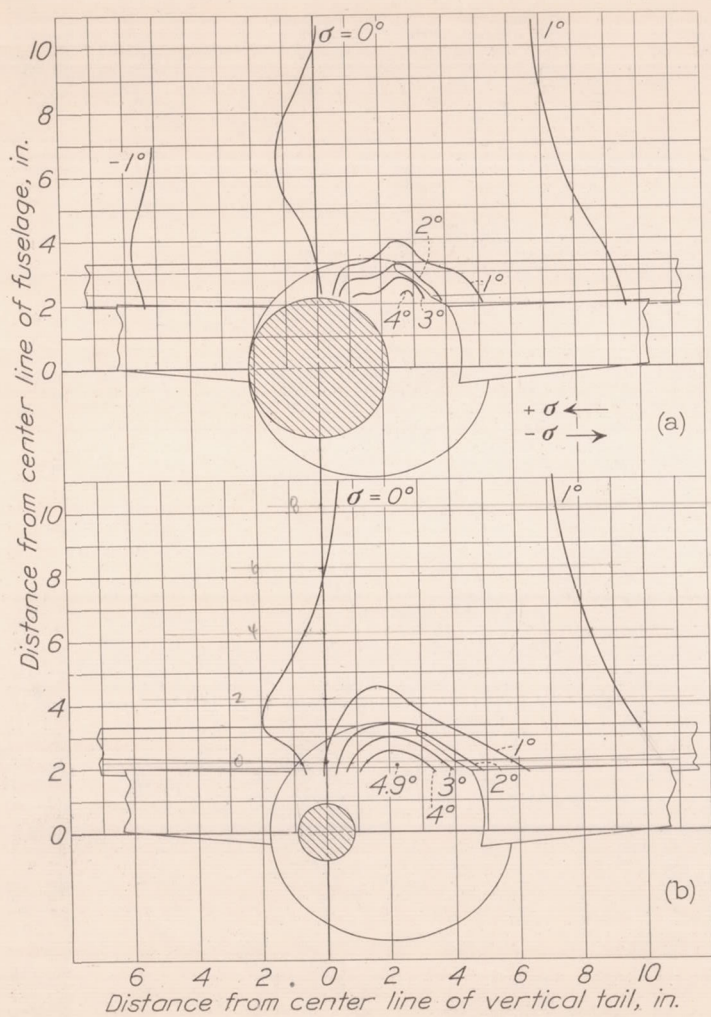
(a) Plane A.   (b) Plane B.
Figure 10.- α = 0°; ψ' = 5°, high wing; δ_f = 60°.
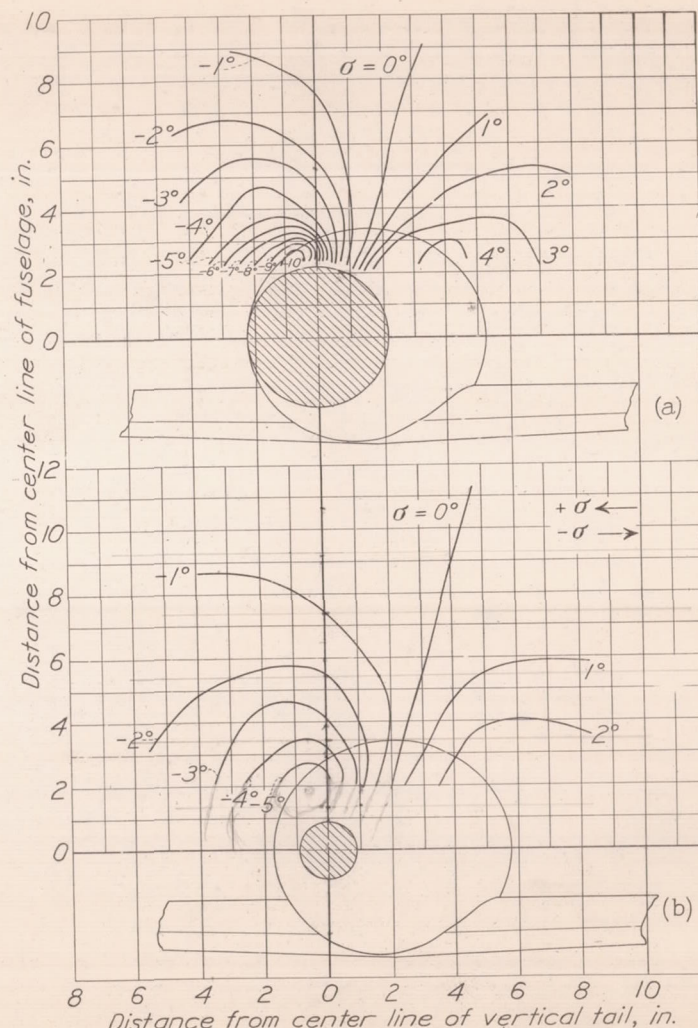
(a) Plane A.   (b) Plane B.
Figure 11.- α = 0°; ψ' = 5°; low wing; δ_f = 0°.

Figures 10,11.- Contours of sidewash angle, σ, in region of tail.

(a) Plane A.
(b) Plane B.
Figure 12.- α = 0°; ψ'= 5°; low wing; δ_f = 60°.

(a) Plane A.
(b) Plane B.
Figure 13.- α = 0°; ψ'= 0°; wing alone; δ_f = 60°.
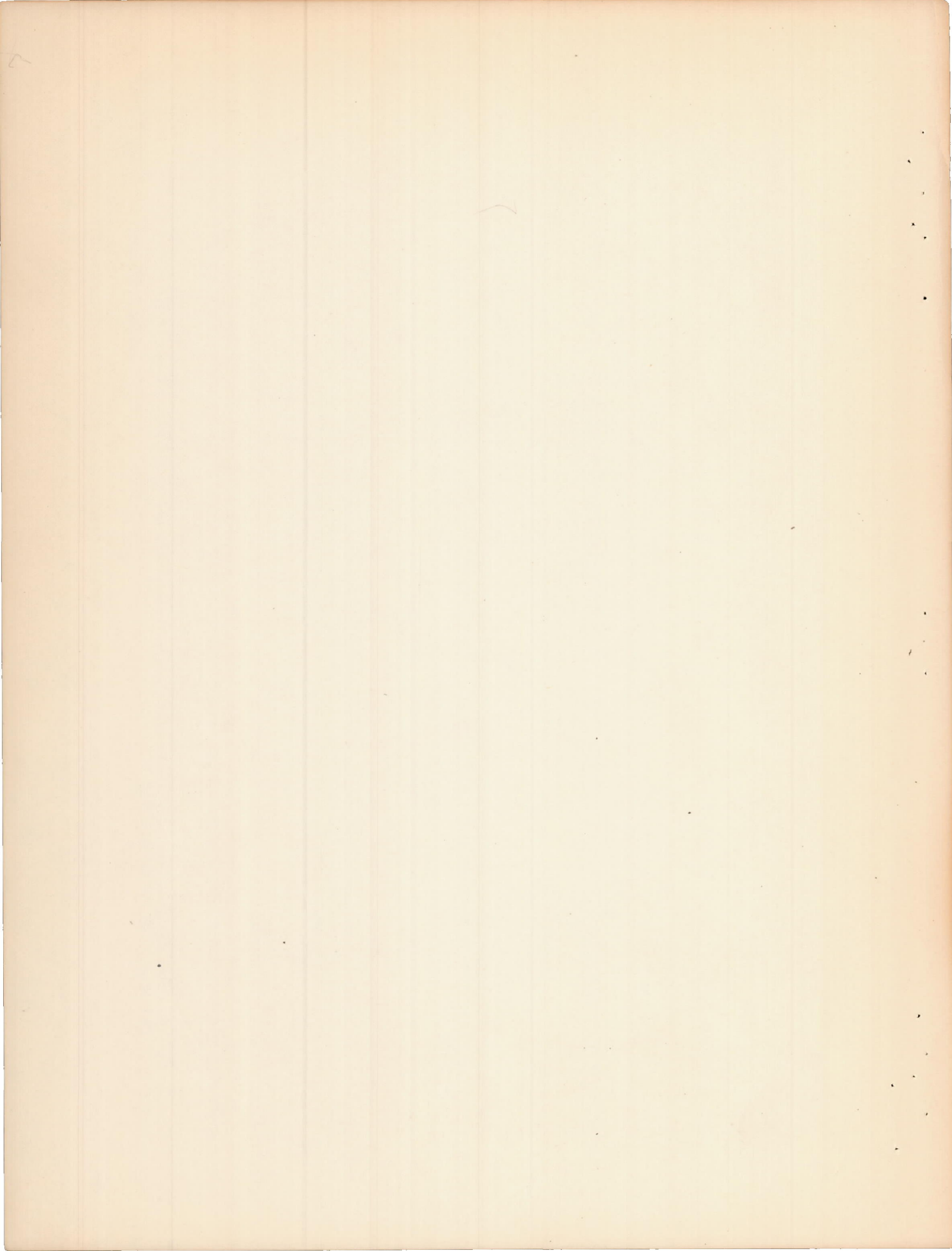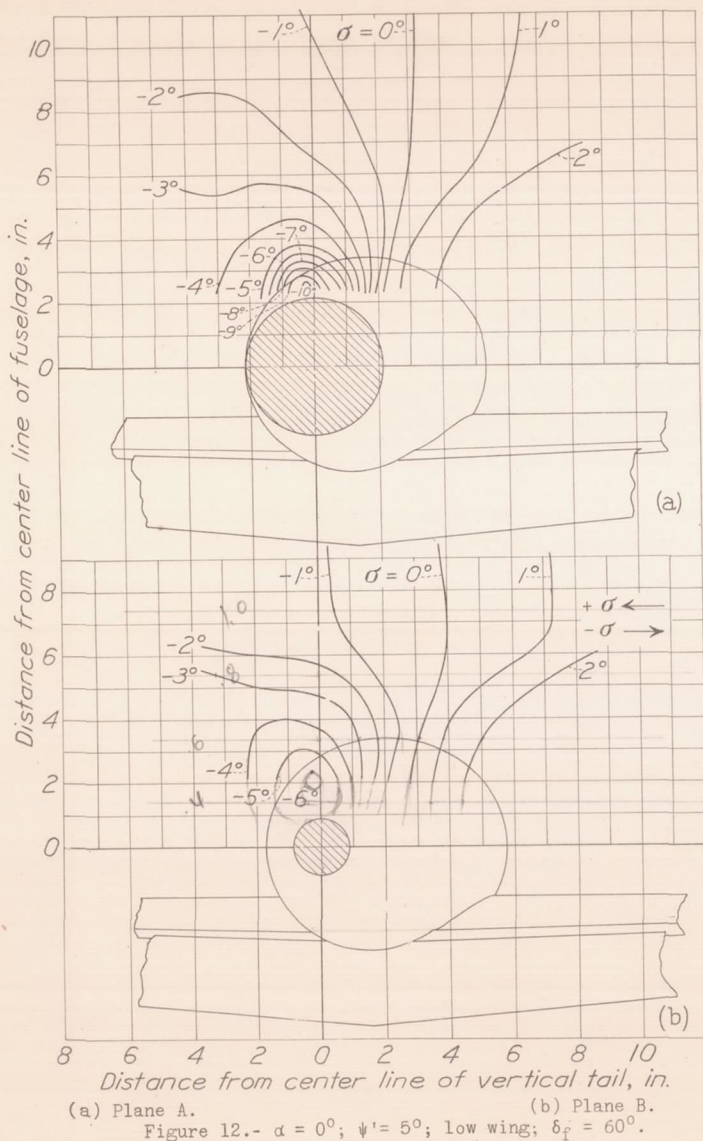
Figures 12,13.- Contours of sidewash angle, σ , in region of tail.
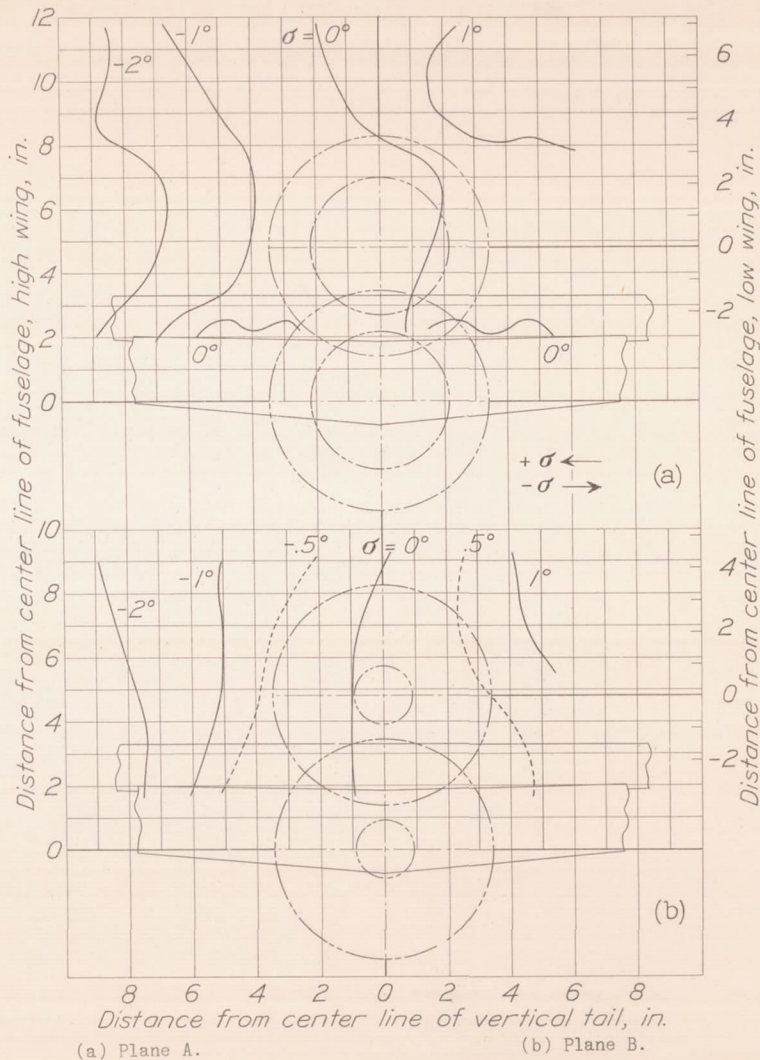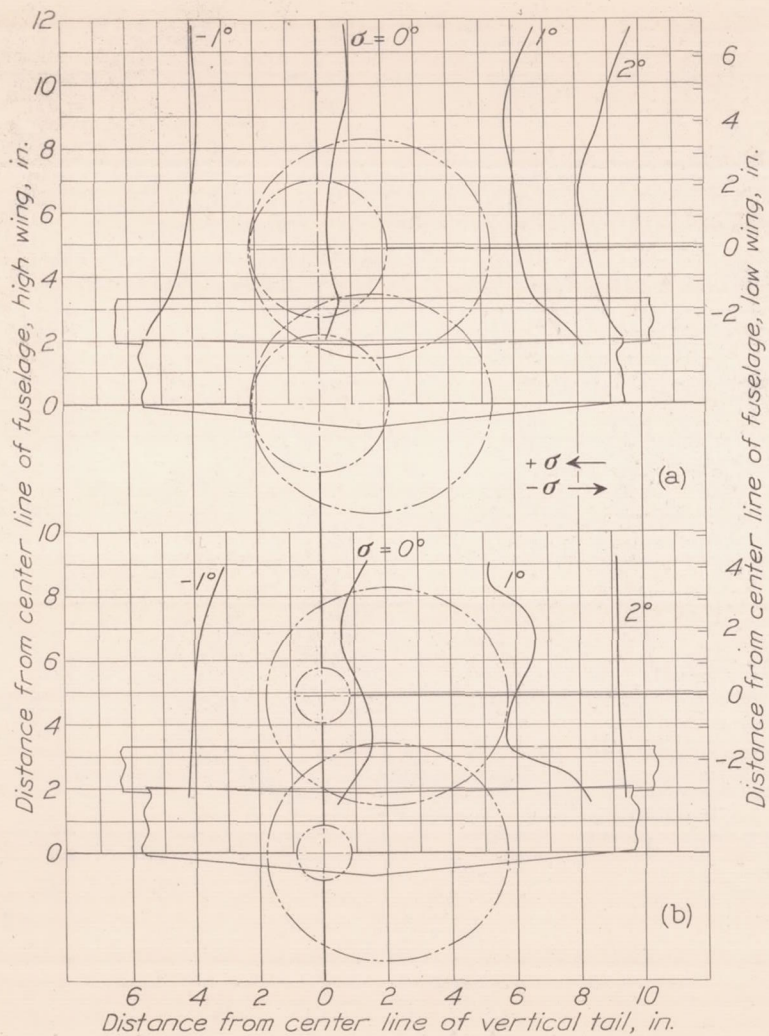
(a) Plane A.

(b) Plane B

Figure 14.- $\alpha = 0°$; $\psi' = 5°$; wing alone; $\delta_f = 60°$.

(a) Plane A.

(b) Plane B.

Figure 15.- $\alpha = 0°$; $\psi' = 0°$; fuselage alone.

Figures 14,15.- Contours of sidewash angle, σ, in region of tail.

(a)

(b)

(a) Plane A. (b) Plane B.

Figure 16.- Contours of sidewash, σ , in region of tail.
α = 0°; ψ'= 5°; fuselage alone.
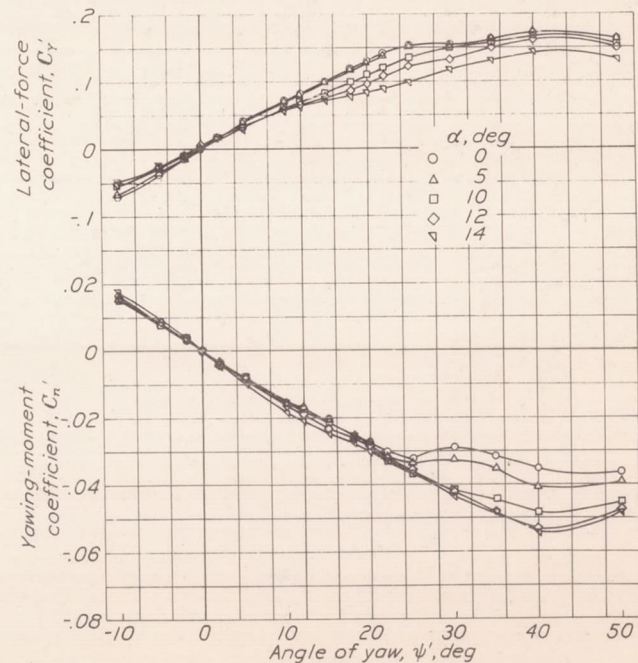
Figure 17.- Yawing-moment and lateral-force
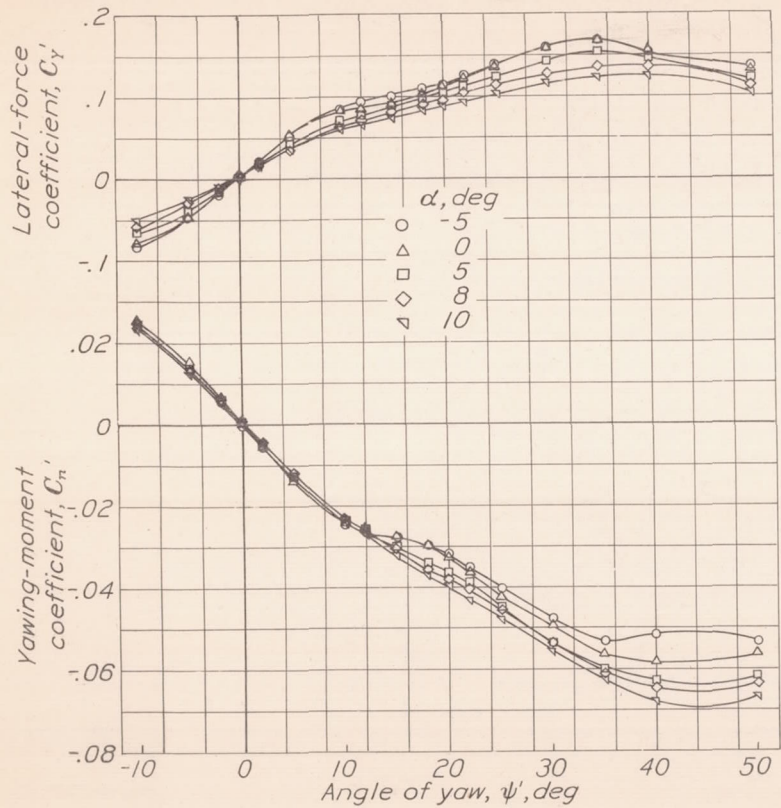coefficients for low-wing combination
with tail. $\delta_f = 0°$.
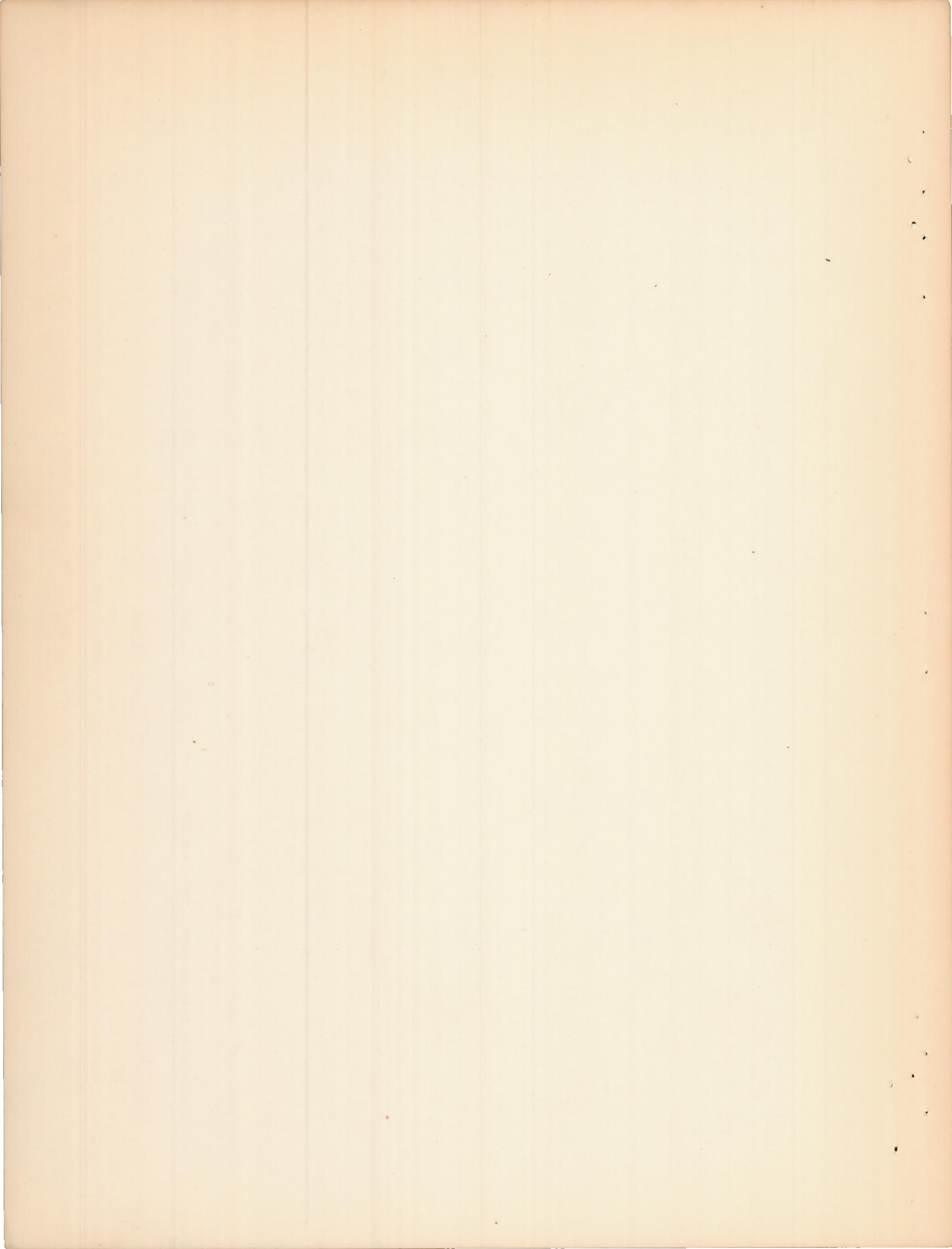
Figure 18.- Yawing-moment and lateral-force coefficients for low-wing combination with tail. $\delta_f = 60^o$.

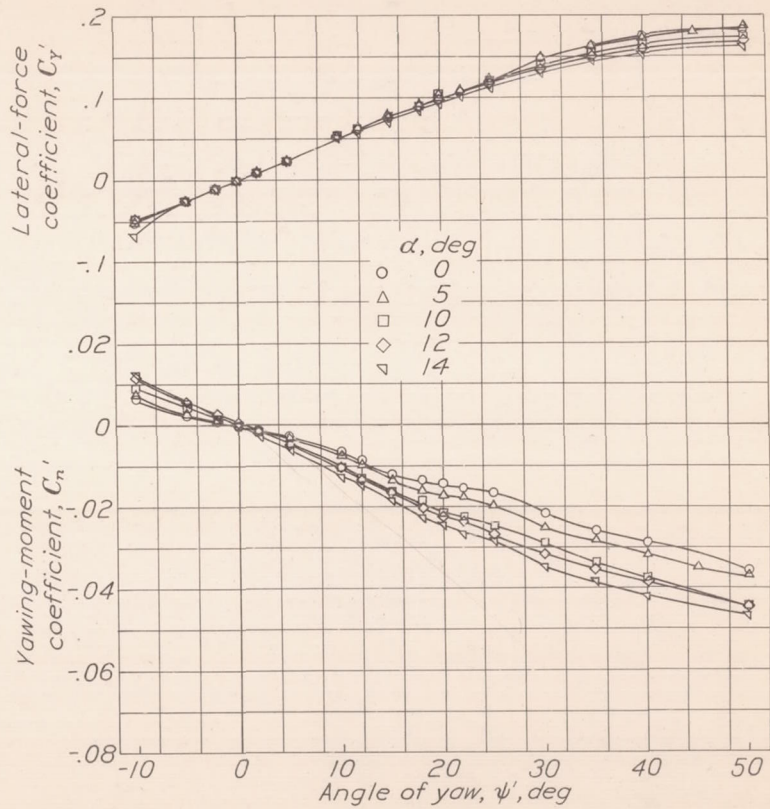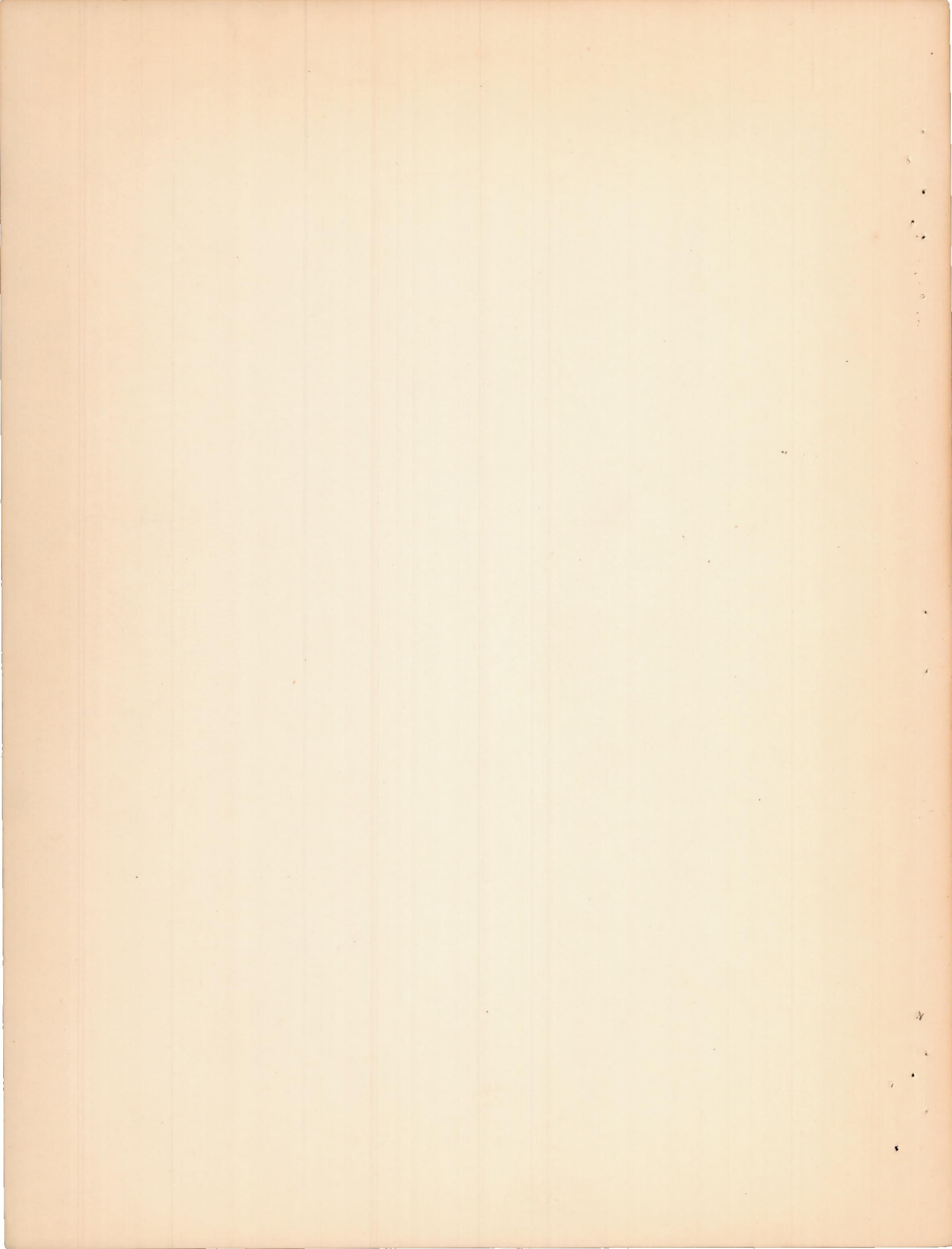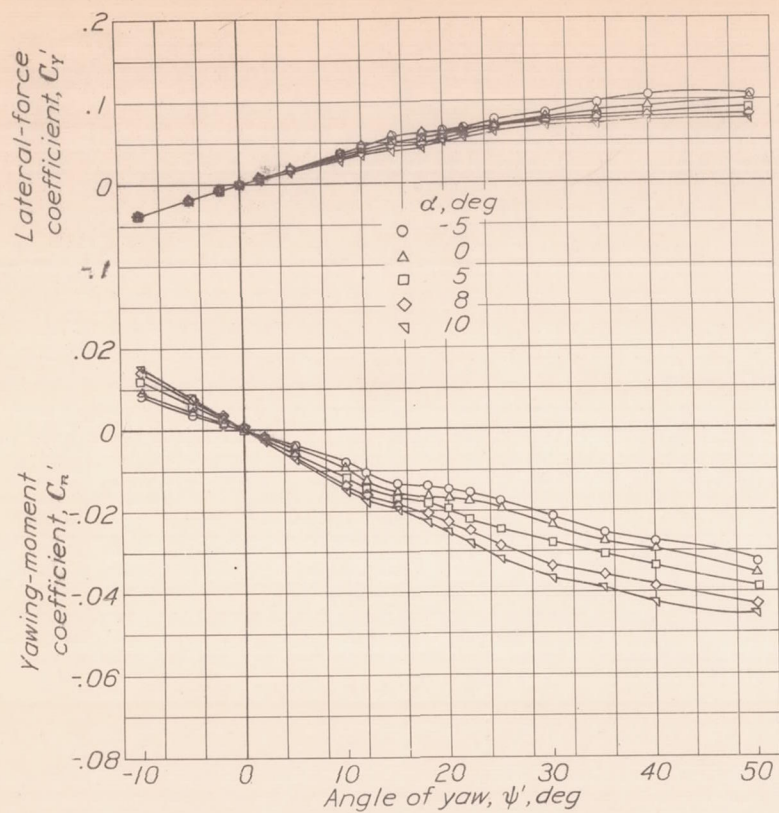Figure 19.- Yawing-moment and lateral-force coefficients for high-wing combination with tail. $\delta_f = 0^o$.

Figure 20.- Yawing-moment and lateral-force
coefficients for high-wing
combination. $\delta_f = 60^o$.

Figure 21.- Sidewash angles at high angles of yaw
on line through rudder hinge, 2.26
inches above fuselage center line. $\alpha = 0^o$; low wing.

(a) $\delta_f = 0^o$. (b) $\delta_f = 60^o$